Zbigniew KACZMARCZYK, Michał ZELLNER

Silesian University of Technology, Department of Power Electronics, Electrical Drives and Robotics

doi:10.15199/48.2020.07.05

Wireless power transfer with almost constant output voltage at variable load

***Abstract**. A concept, selected properties and a design method of wireless power transfer (WPT) systems with almost constant output voltage at variable load are presented in the paper. The proposed solution has no feedback, and at the same time allows to adjust the ratio of the output voltage to the input voltage despite the use of identical magnetically coupled coils. A theoretical background and an experimental verification are included.*

Streszczenie.** W artykule przedstawiono koncepcję, wybrane właściwości i metodę projektowania układów bezprzewodowego przesyłu energii (WPT - wireless power transfer) elektrycznej z prawie niezmiennym napięciem wyjściowym przy zmiennym obciążeniu. Zaproponowane rozwiązanie nie posiada sprzężeń zwrotnych oraz jednocześnie pozwala na dostosowanie stosunku między napięciem wyjściowym a napięciem wejściowym pomimo zastosowania identycznych cewek sprzężonych magnetycznie. Zamieszczono podstawy teoretyczne i eksperymentalną weryfikację.* ***(Bezprzewodowy przesył energii elektrycznej z prawie niezmiennym napięciem wyjściowym przy zmiennym obciążeniu)

Keywords: wireless power transfer (WPT), coupled coils, resonant circuits
Słowa kluczowe: bezprzewodowy przesył energii (WPT), cewki sprzężone, obwody rezonansowe

Introduction

Currently, due to obvious advantages, wireless power transfer (WPT) systems are becoming more and more popular. They are applied in many devices, such as: chargers, implants and robots [1]. The most common method of the WPT is the use of the inductive coupling (e.g. [2]). This paper discusses selected issues considering inductive WPT systems with almost constant output voltage at the variable load.

A design method of basic WPT systems operating with the optimal efficiency for a given load is introduced in [3]. Unfortunately, such systems are susceptible to load changes and do not stabilize the output voltage. The solution of this problem is the design of more advanced controlled systems or the use of other design methods (or other topologies).

In controlled systems various strategies are applied. For example, frequency control [4] or PWM control [5] can be used to change the output power. In [6], the authors propose connecting an additional converter at the output of the WPT system in order to control transferred power. However, the converter reduces the overall efficiency and generates additional harmonics. Searching for solutions that tolerate load changes leads to testing other WPT systems. Basic topologies [7] with conventional design methods require a dedicated control. Other topologies, such as LCC [8] or LCL-N [9], require the use of specific design methods that enable shaping WPT system characteristics. Some topologies, such as cascades of magnetically coupled coils [10], are even more susceptible to load changes, but have a significant advantage (higher energy transfer efficiency over longer distances). The last group of topologies are WPT systems with switched capacitors, e.g. [11].

The principle of operation, selected properties, design method and results of laboratory tests of the series-series (s-s) WPT system with almost constant output voltage at load changes are presented in the paper. The proposed concept is very simple, without the need for additional control.

Principle of operation

To explain the concept of the series-series (s-s) WPT system with almost constant output voltage at the variable load, two schematics of magnetically coupled coils are discussed and compared (Fig. 1). For simplicity, the considerations relate to the fundamental harmonic (the complex analysis).

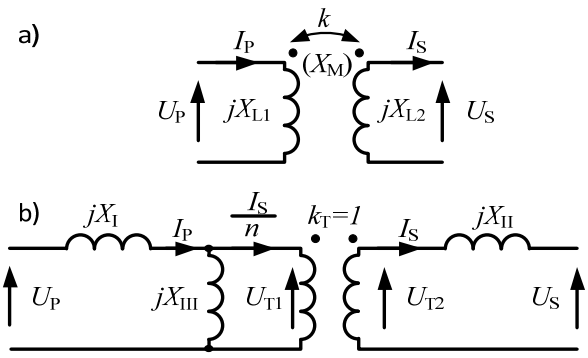

Fig.1. Schematics of coupled coils: a) general, b) extended

A general schematic of coupled coils (Fig. 1a) is built with two reactances (X_{L1}, X_{L2}), and a coupling coefficient k (a mutual reactance X_M). It is described with the set of equations:

$$\begin{cases} U_P = jX_{L1}I_P - jk\sqrt{X_{L1}X_{L2}}I_S \\ U_S = jk\sqrt{X_{L1}X_{L2}}I_P - jX_{L2}I_S \end{cases}. \tag{1}$$

The coupling coefficient k is defined as:

$$k = \frac{X_M}{\sqrt{X_{L1}X_{L2}}}. \tag{2}$$

An extended schematic of coupled coils (Fig. 1b) is built with three reactances (X_I, X_{II}, X_{III}) and an ideal transformer ($k_T = 1$) with a transformation ratio n. This schematic is described as:

$$\begin{cases} U_P = j(X_I + X_{III})I_P - jX_{III}\dfrac{I_S}{n} \\ U_S = j\dfrac{X_{III}}{n}I_P - j(\dfrac{X_{III}}{n^2} + X_{II})I_S \end{cases}, \tag{3}$$

$$n = \frac{U_{T1}}{U_{T2}}, \tag{4}$$

where U_{T1}, U_{T2} are voltages of the ideal transformer.

The case of equivalence of two schematics ((1) and (3)) leads to the following conditions:

$$\begin{cases} X_{L1} = X_I + X_{III} \\ k\sqrt{X_{L1}X_{L2}} = \dfrac{X_{III}}{n} \\ X_{L2} = \dfrac{X_{III}}{n^2} + X_{II} \end{cases} \tag{5}$$

which can be simplified to:

$$\begin{cases} X_I = X_{L1} - nk\sqrt{X_{L1}X_{L2}} \\ X_{II} = X_{L2} - \dfrac{k}{n}\sqrt{X_{L1}X_{L2}} \end{cases}. \tag{6}$$

It should be noted that the transformation ratio n can be assumed arbitrarily, and its value determines the reactances X_I and X_{II} for known X_{L1}, X_{L2} and k.

In order to achieve a constant output voltage at the variable load, additional components should compensate for reactances X_I and X_{II}. In the case of passive components connected in series, they are calculated as negative values of jX_I and jX_{II}. This is called as a s-s compensation and it is shown in Fig. 2.

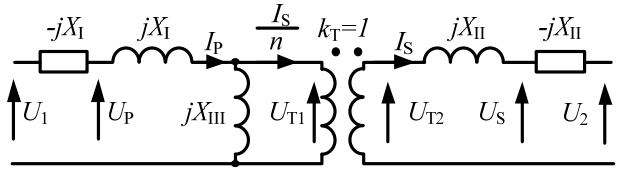

Fig. 2. Extended schematic of coupled coils with s-s compensation

In the conditions of the s-s compensation (Fig. 2), equation (4) can be extended to:

$$n = \frac{U_{T1}}{U_{T2}} = \frac{U_1}{U_2}. \tag{7}$$

It is seen that input and output voltages are depended only on the ratio n. Its value can be given almost arbitrarily even for the same reactances X_{L1} and X_{L2}.

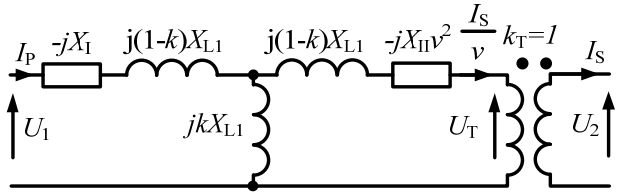

Fig.3. Schematic of coupled coils with the s-s compensation and the transformer T-model

In the next step, the third equivalent schematic of coupled coils is introduced (Fig. 3). It is created using the presented the s-s compensation and well-known transformer T-model with a transformation ratio v, defined as:

$$\nu = \frac{U_T}{U_2} = \sqrt{\frac{X_{L1}}{X_{L2}}}. \tag{8}$$

As a consequence, a compensation ratio μ is given as:

$$\mu = \frac{n}{\nu} = \frac{U_1}{U_T}. \tag{9}$$

Finally, the total ratio n (7) is the product of above ratios v (8) and μ (9). The first one is depended on reactances X_{L1} and X_{L2}, and the second on compensation parameters. Equations (6) can be rewritten as:

$$\begin{cases} X_I = X_{L1}(1-\mu k) \\ X_{II} = X_{L2}\left(1 - \dfrac{k}{\mu}\right) \end{cases} \tag{10}$$

For the schematic shown in Fig. 3 loaded with a resistor R, an equivalent input circuit can be created (Fig. 4). The resistor R represents an output rectifier and its DC load. It is seen that the transformed reactance and transformed load are connected directly to the power supply. If the compensation ratio μ is greater than zero, the input impedance is inductive. This case is preferred for supplying the circuit with voltage inverters.

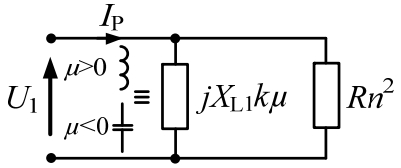

Fig. 4. Equivalent input impedance circuit

To simplify further analysis, conditions that should be met for the inductive or capacitive type of compensation reactances are summarized in table 1. The conditions depend on the coupling coefficient k and the compensation ratio μ. The table also shows that both reactances cannot be inductive at the same time.

Table 1. Types of compensation reactances

	$X_I < 0$ (inductive)	$X_I = 0$	$X_I > 0$ (capacitive)
$X_{II} < 0$ (inductive)	–	–	$k > \mu > 0$ Ⓑ
$X_{II} = 0$	–	$k = 1 \wedge \mu = 1$	$\mu = k$
$X_{II} > 0$ (capacitive)	$\mu > \dfrac{1}{k}$ Ⓐ	$\mu = \dfrac{1}{k}$	$\mu < 0 \cup \dfrac{1}{k} > \mu > k$ Ⓒ

Equations (10) can be presented as parametric plots (Fig. 5), eliminating μ (the first equation) and k (the second equation), respectively:

$$\begin{cases} \dfrac{X_{II}}{X_{L2}} = \dfrac{k^2}{\dfrac{X_I}{X_{L1}} - 1} + 1 \\ \dfrac{X_{II}}{X_{L2}} = \dfrac{1}{\mu^2}\left(\dfrac{X_I}{X_{L1}} - 1\right) + 1 \end{cases}. \tag{11}$$

The specific compensation reactances are found as the intersection of straight lines and hyperboles (Fig. 5) from equation (11).

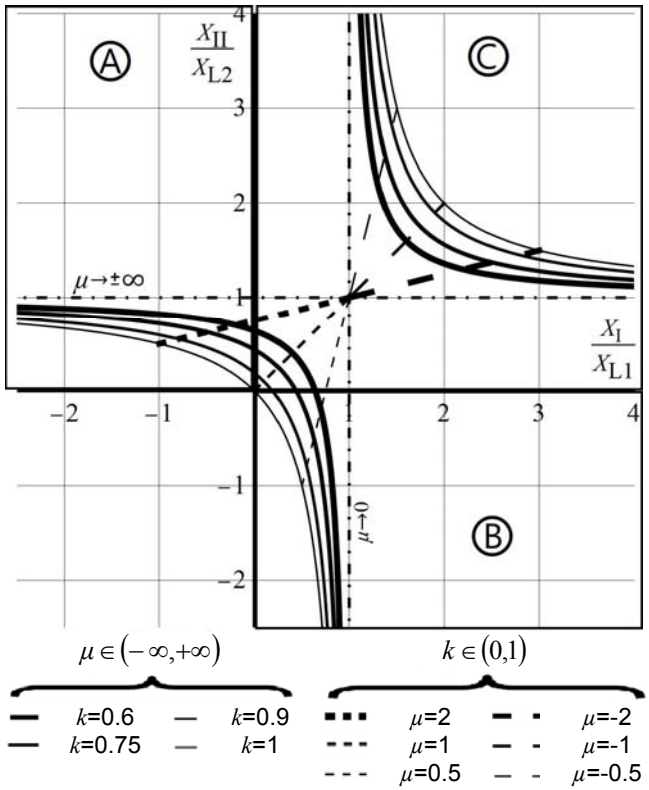

Fig.5. Characteristics of relative compensation reactances

Optimisation of efficiency

The schematics discussed earlier are lossless. Thus, power losses and the efficiency can only be estimated, assuming that parasitic resistances have a negligible effect on calculated currents. Power losses are given as follows:

$$P_{\text{loss}}=\begin{cases} R_{\text{L}}(I_{\text{P}}I_{\text{P}}'+I_{\text{S}}I_{\text{S}}')+R_{\text{I}}I_{\text{P}}I_{\text{P}}' & \text{, for Table 1 - Ⓐ,} \\ R_{\text{L}}(I_{\text{P}}I_{\text{P}}'+I_{\text{S}}I_{\text{S}}')+R_{\text{II}}I_{\text{S}}I_{\text{S}}' & \text{, for Table 1 - Ⓑ,} \\ R_{\text{L}}(I_{\text{P}}I_{\text{P}}'+I_{\text{S}}I_{\text{S}}') & \text{, for Table 1 - Ⓒ,} \end{cases} \tag{12}$$

where R_{L} is a coil resistance of the WPT system, R_{I} and R_{II} are resistances of inductive compensation components. For simplicity, it is assumed that magnetically coupled coils are identical ($v=1$) and power losses of capacitive compensation components are negligible.

In order to have a general representation, relative parameters (marked with dot) are introduced. Reference parameters are U_1 and R, obtaining:

$$\dot{X}_{\text{L}}=\frac{X_{\text{L1}}}{R}=\frac{X_{\text{L2}}}{R}. \tag{13}$$

$$\dot{I}_{\text{P}}=\frac{I_{\text{P}}R}{U_1}, \tag{14}$$

$$\dot{I}_{\text{S}}=\frac{I_{\text{S}}R}{U_1}=\frac{U_2}{U_1}=\frac{1}{\mu}. \tag{15}$$

For the equivalent input circuit (Fig. 4), the primary-side current is given by:

$$\dot{I}_{\text{P}}=-\frac{j}{\dot{X}_{\text{L}}\mu k}+\frac{1}{\mu^2}. \tag{16}$$

Next, quality factors are introduced:

$$Q_L=\frac{X_{\text{L1}}}{R_{\text{L}}}=\frac{X_{\text{L2}}}{R_{\text{L}}}=\frac{\dot{X}_{\text{L}}}{\dot{R}_{\text{L}}}, \tag{17}$$

$$Q_{\text{I}}=\frac{X_{\text{I}}}{R_{\text{I}}}=\frac{X_{\text{L1}}(\mu k-1)}{R_{\text{I}}}=\frac{\dot{X}_{\text{L}}(\mu k-1)}{\dot{R}_{\text{I}}}, \tag{18}$$

$$Q_{\text{II}}=\frac{X_{\text{II}}}{R_{\text{II}}}=\frac{X_{\text{L1}}(\frac{k}{\mu}-1)}{R_{\text{II}}}=\frac{\dot{X}_{\text{L1}}(\frac{k}{\mu}-1)}{\dot{R}_{\text{II}}}. \tag{19}$$

For the case Table 1 - Ⓐ, power losses and the efficiency can be calculated as:

$$\dot{P}_{\text{loss\_A}}=\left(\frac{\dot{X}_{\text{L}}}{Q_{\text{L}}}+\frac{\dot{X}_{\text{L}}(\mu k-1)}{Q_{\text{I}}}\right)\left(\frac{1}{\mu^4}+\frac{1}{\dot{X}_{\text{L}}^{\,2}k^2\mu^2}\right)+\frac{\dot{X}_{\text{L}}}{Q_{\text{L}}}\frac{1}{\mu^4} \tag{20}$$

$$\dot{\eta}_{\text{A}}=1-\dot{P}_{\text{loss\_A}}\mu^2= \tag{21}$$
$$=1-\left(\left(\frac{\dot{X}_{\text{L}}}{Q_{\text{L}}}+\frac{\dot{X}_{\text{L}}(\mu k-1)}{Q_{\text{I}}}\right)\left(\frac{1}{\mu^2}+\frac{1}{\dot{X}_{\text{L}}^{\,2}k^2}\right)+\frac{\dot{X}_{\text{L}}}{Q_{\text{L}}}\frac{1}{\mu^2}\right).$$

Comparing the derivative of the given efficiency to zero, the optimal relative reactance is found:

$$\dot{X}_{\text{Lopt\_A}}=\frac{\mu}{k}\sqrt{\frac{(\mu k-1)Q_{\text{L}}+Q_{\text{I}}}{(\mu k-1)Q_{\text{L}}+2Q_{\text{I}}}}. \tag{22}$$

For the optimal reactance, the maximal efficiency is obtained:

$$\eta_{\text{opt\_A}}=1-\frac{2\sqrt{((\mu k-1)Q_{\text{L}}+Q_{\text{I}})((\mu k-1)Q_{\text{L}}+2Q_{\text{I}})}}{Q_{\text{L}}Q_{\text{I}}k\mu}. \tag{23}$$

Analogous calculations are carried out for the case Table 1 - Ⓑ:

$$\dot{X}_{\text{Lopt\_B}}=\frac{\mu}{k}\sqrt{\frac{Q_{\text{II}}}{\left(\frac{k}{\mu}-1\right)Q_{\text{L}}+2Q_{\text{II}}}}, \tag{24}$$

$$\eta_{\text{opt\_B}}=1-\frac{2}{Q_{\text{L}}k\mu}\sqrt{\frac{\left(\frac{k}{\mu}-1\right)Q_{\text{L}}+2Q_{\text{II}}}{Q_{\text{II}}}}. \tag{25}$$

The last case (Table 1 - Ⓒ) can be presented as the limit of the case Table 1 - Ⓐ for $Q_{\text{I}}\to+\infty$ (or the case Table 1 - Ⓑ for $Q_{\text{II}}\to+\infty$):

$$\dot{X}_{\text{Lopt\_C}}=\sqrt{\frac{1}{2}}\frac{\mu}{k}, \tag{26}$$

(27) $$\eta_{\text{opt\_C}} = 1 - \frac{2\sqrt{2}}{k\mu}.$$

As an example, assuming k_T = 0,8, Q_L = 100, Q_I = Q_{II} = 200, 100, 10, the optimal relative reactances and maximal efficiencies are presented in Fig. 6 and Fig. 7, respectively. Individual cases relating to Table 1 are marked. The assumed values are representative of the available on the market elements, especially considering the power range and size of the laboratory WPT system. It is seen that results strongly depend on the compensation ratio μ and less on quality factors Q_I and Q_{II}.

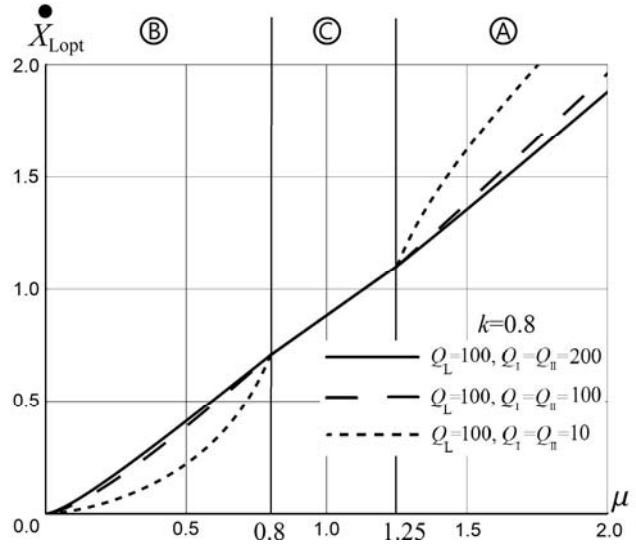

Fig.6. Optimal relative reactances as a function of the ratio μ

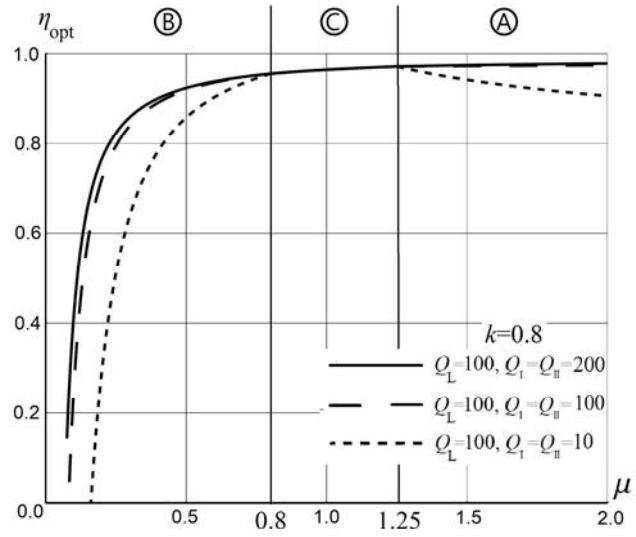

Fig.7. Maximal efficiencies as a function of the ratio μ

Design method

The presented equations can be formed into the design method of s-s compensated WPT systems (Fig. 8).

Firstly, some initial data are assumed. The algorithm can be used several times, setting initial data more and more accurately at each step.

Next, after determining the compensation type (Table 1. - Ⓐ, Ⓑ or Ⓒ), the quality factor of the compensation component is introduced and the optimal coil reactance is calculated.

Now, compensation reactances are found. Output data and the operating frequency are used to calculate WPT system inductances and capacitances. Finally, obtained system parameters can be verified experimentally.

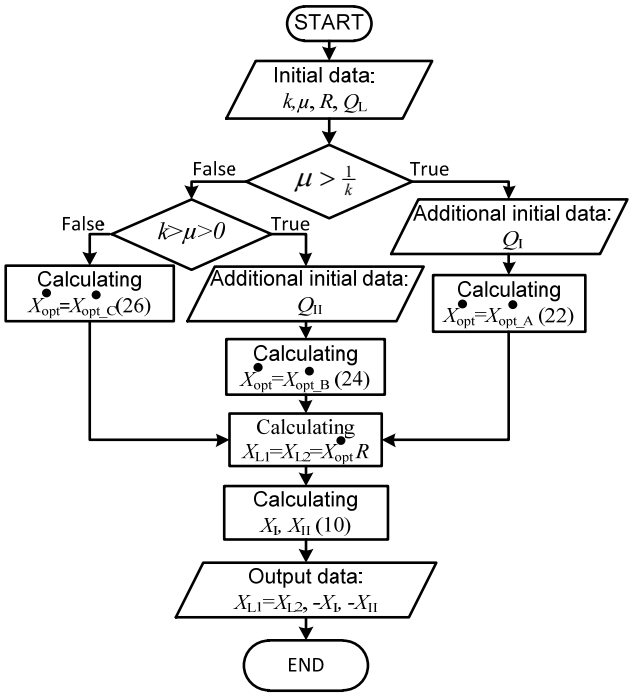

Fig.8. Design method

Experimental results

Laboratory WPT system was designed to deliver the output power of 100 W at the frequency of 100 kHz, the DC input voltage of 50 V and the DC output voltage of 12 V (Fig. 9). It was built with two identical coupled coils of 50 mm in diameter (v = 1) - WE-WPCC series manufactured by Würth Elektronik. The system is powered from the voltage inverter, containing four AOB2500L N-channel MOSFET transistors (U_{DS} = 150 V, $R_{DS(on)}$ < 6,5 mΩ). Its output is connected to the full-bridge rectifier with the variable resistor R_{var}. Four DSA60C45PB Schottky diodes (U_{RRM} = 45 V, I_{FAV} = 30 A) and a set of capacitors connected in parallel (C_{out} = 40 mF) form the rectifier.

a)

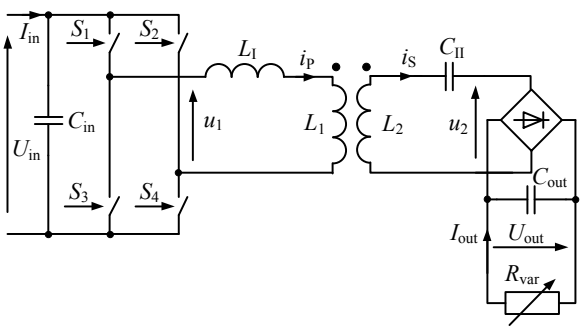

b)

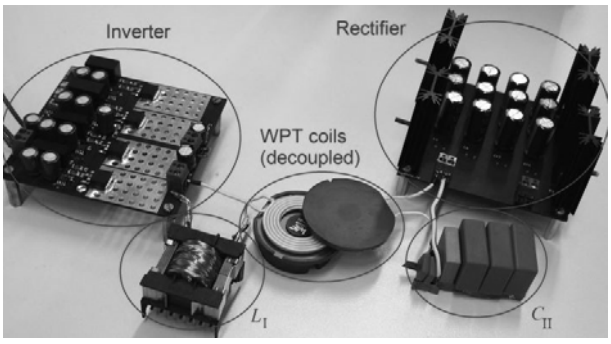

Fig.9. Laboratory WPT system: a) schematic, b) general view

The parameters of the laboratory WPT system were determined using the presented design method (Fig. 8). The equivalent AC load resistance R was 1,2 Ω, and considering parasitic resistances, the compensation ratio μ was 3,85 (50 V / 13 V = 3,85) instead of 4,17 (50 V / 12 V = 4,17). The other parameters were measured with Agilent 4294A impedance analyser or were estimated based on data sheets. They are summarized in Table 2.

Table 2. Parameters of the laboratory WPT system

Name	Symbol	Value	Additional information
Inductance of coupled coils	L_1, L_2	8,7 μH	Manufacturer: Würth Elektronik
Inductance of primary-side compensation component	L_{I}	19,4 μH	Built with N87 material
Capacitance of secondary-side compensation component	C_{II}	370 nF	Manufacturer: Würth Elektronik (foil capacitors)
Coupling coefficient	k	0,84	Measured
Quality factor of coupled coils	Q_{L}	100	Measured
Quality factor of primary-side compensation component	Q_{I}	60	Estimated from material characteristics

The representative oscillograms of the laboratory WPT system are presented in Fig. 10. They were measured with the Agilent MSO6034A oscilloscope equipped with 10074C voltage and N2774A current probes. It is seen that the primary-side u_1 and secondary-side u_2 voltages are rectangular. The primary-side current i_{P} is triangular for the low load condition (high output resistance - Fig. 10a) and close to sinusoidal for the rated load condition (optimal output resistance - Fig. 10b). The secondary-side current i_{S} is sinusoidal.

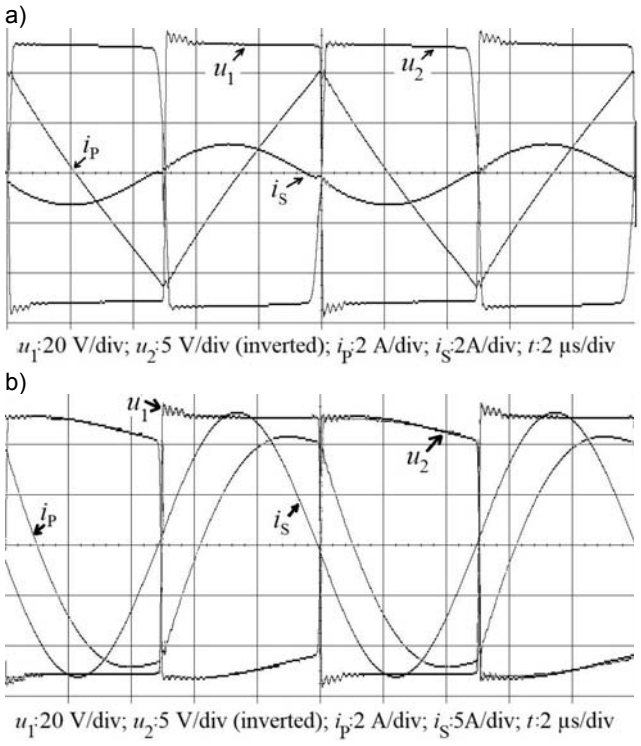

Fig.10. Laboratory WPT system oscillograms: a) low load condition (R_{var} = 17 Ω), b) rated load condition (R_{var} = 1,44 Ω)

The measured output U_{out} and average absolute input U_2 voltages of the rectifier for variable load are given in Fig. 11. Additionally, the calculated voltage $U_{2\mathrm{cal}}$ is included. The calculations were performed in a similar way as described in the chapter “Optimalization of efficiency”. The voltages, as expected, are almost constant. They change due to parasitic resistances of WPT system components. Moreover, the output voltage U_{out} depends on the voltage drop on Schottky diodes of the rectifier. It can be partially compensated by using controlled MOSFET transistors instead of diodes.

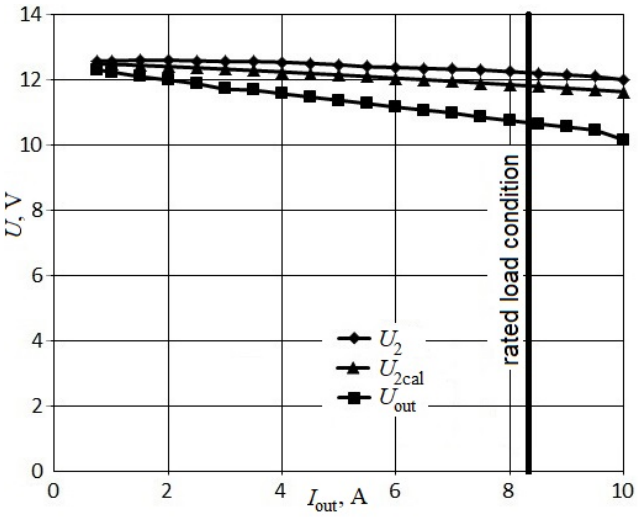

Fig.11. Secondary-side voltages of the laboratory WPT system

The WPT system efficiencies are drawn in Fig. 12. The DC-DC characteristic shows the overall efficiency, while the AC-AC characteristic skips power losses of converters. The third characteristic is calculated based on approximate equations discussed in the paper.

Considering theoretical and experimental results, it should be explained that the proposed design method requires additional studies. At the first step, the exact insertion of parasitic resistances is advisable. Next, more complex analysis is needed, taking into account higher harmonics and different magnetically coupled coils.

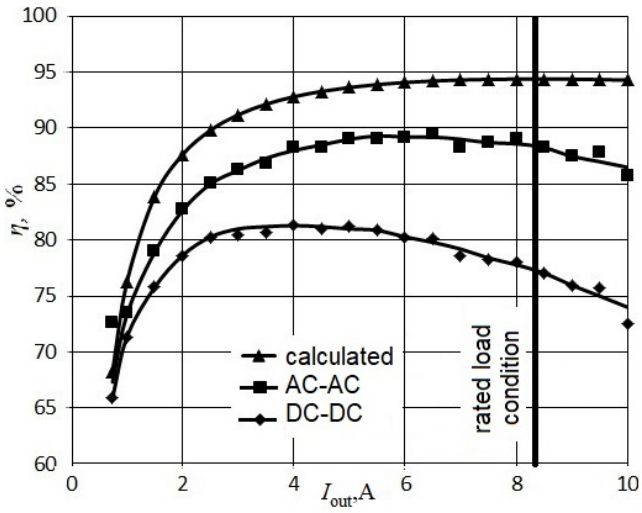

Fig.12. Laboratory WPT system efficiencies

Conclusions

The paper presents selected properties and the design method of WPT systems with almost constant output voltage at variable load. It was explained theoretically and verified experimentally, that such systems can be realised by the appropriate series-series compensation of two magnetically coupled coils. The considered systems operate without the control and enable obtaining a given ratio of the output voltage to the input voltage almost independently of the reactances of the coupled coils. However, the total voltage ratio is the product of the transformation ratio (depending on reactances X_{L1} and X_{L2}) and the compensation ratio (depending on compensation reactances X_I and X_{II}). Reactances X_{L1} and X_{L2} are related to the load resistance R, ensuring the high efficiency. Compensation reactances X_I and X_{II} are associated with maintaining a constant output voltage.

The laboratory WPT system with almost constant output voltage at variable load was built and tested. The experimental verification confirmed the proposed concept, but at the same time pointed out some disadvantages - too simplified the design method and significant influence of the rectifier. As a continuation, the design method and the rectifier will be improved.

***Authors**: Zbigniew Kaczmarczyk, D.Sc., Eng., Prof. of SUT, Michał Zellner M.Sc. Eng., Silesian University of Technology, Department of Power Electronics, Electrical Drives and Robotics, ul. B. Krzywoustego 2, 44-100 Gliwice.*
E-mails: Zbigniew.Kaczmarczyk@polsl.pl, Michal.Zellner@polsl.pl.

REFERENCES

[1] Moradewicz A., Kaźmierkowski M.P., Unplugged but connected: Review of Contactless Energy Transfer Systems, *IEEE Industrial Electronics Magazine*, 6 (2012), No. 4, 47-55, ISSN: 1941-0115, DOI: 10.1109/MIE.2012.2220869

[2] Moradewicz A., On / Off - board chargers for electric vehicles, *Przegląd Elektrotechniczny*, 95 (2019), nr 2, str. 136-139, ISSN 0033-2097, DOI:10.15199/48.2019.02.30

[3] Cieśla T., Kaczmarczyk Z., Grzesik B., Stępień M., Obwody do przesyłu bezprzewodowego energii elektrycznej, *Elektryka*, 212 (2009), Zeszyt 4

[4] Patil D., Sirico M., Gu L., Fahimi B., Maximum efficiency tracking in wireless power transfer for battery charger: Phase shift and frequency control, *2016* IEEE Energy Conversion Congress and Exposition (ECCE), 1-8, ISBN: 978-1-5090-0737-0, DOI: 10.1109/ECCE.2016.7855234

[5] Yang Y., Zhong W., Tan S., Ron Hui S.Y., Dynamic improvement of wireless power transfer systems with maximum energy efficiency tracking by sliding mode control, 2017 IEEE 3rd International Future Energy Electronics Conference and ECCE Asia (IFEEC *2017 - ECCE Asia),* 1736-1740, ISBN: 978-1-5090-5157-1, DOI: 10.1109/IFEEC.2017.7992310

[6] Zhong W., Ron Hui S.Y., Charging time control of wireless power transfer systems without using mutual coupling information and wireless communication system, *IEEE Transactions on Industrial Electronics*, 64 (2017), No. 1, 228-235, ISSN: 1557-9948, DOI: 10.1109/TIE.2016.2598725

[7] Sîrbu I., Mandache L., Comparative analysis of different topologies for wireless power transfer systems, 2017 IEEE International Conference on Environment and Electrical Engineering and 2017 IEEE Industrial and Commercial Power Systems Europe (EEEIC / I&CPS Europe), 1-6, ISBN: 978-1-5386-3917-7, DOI: 10.1109/EEEIC.2017.7977863

[8] Ramezani A., Farhangi S., Iman-Eini H., Farhangi B., Rahimi R., Moradi G., Optimized LCC-Series Compensated Resonant Network for Stationary Wireless EV Chargers, *IEEE Transactions on Industrial Electronics*, 66 (2019), No. 4, 2756-2765, ISSN: 1557-9948, DOI: 10.1109/TIE.2018.2840502

[9] Zhang Y., Yan Z., Liang Z., Li S., Mi C., *An* LCL-N Compensated Strongly-Coupled Wireless Power Transfer System for High-Power Applications, *2019* IEEE Applied Power Electronics Conference and Exposition (APEC), 3088-3091, ISSN: 2470-6647, DOI: 10.1109/APEC.2019.8721847

[10] Kaczmarczyk Z., Frania K., Bodzek K., Ruszczyk A., Analiza właściwości rezonansowych kaskad cewek ze względy na zwiększanie odległości przesyłu, *Przegląd Elektrotechniczny*, 94 (2018), nr 12, str. 112-118 ISSN 0033-2097, DOI:10.15199/48.2018.12.24

[11] Han C., Zhang B., Fang Z., Qiu D., Chen Y., Xiao W., Dual-Side Independent Switched Capacitor Control for Wireless Power Transfer with Coplanar Coils, *Energies,* 1472 (2018), No. 11, DOI:10.3390/en11061472